3. V. I. Vladimirov and A. A. Kusov, "Modeling the development kinetics of the dislocation structure near the surface of a crystal," Fiz. Tverd. Tela, 20, No. 10 (1978).
4. A. M. Kosevich and M. L. Polyakov, "Collective oscillations of a dislocation wall," Fiz. Tverd. Tela, 21, No. 10 (1979).
5. J. N. Johnson, O. E. Jones, and T. E. Michaels, "Dislocation dynamics and single-crystal constitutive relation," J. Appl. Phys., 41, No. 6 (1970).
6. A. Ya. Krasovskii, "Damping of elastic shock waves in iron due to viscous retardation of dislocations," Probl. Prochn., No. 7 (1970).
7. A. I. Nedbai, Yu. V. Sud'enkov, et al., "Effect of loading rate on the behavior of elasticoviscoplastic materials," Pis'ma Zh. Tekh. Fiz., 6, No. 18 (1980).
8. Yu. I. Meshcheryakov and V. A. Morozov, "Investigation of the initial stage of dynamic plasticity in A-995 aluminum," ChMMSS, 11, No. 3 (1980).
9. C. S. Smith, Trans. Metall. Society AIME, 212, 574 (1958).
10. J. Weertman, "Dislocation mechanics at high strain rates," in: Metallurgical Efficiencies at High Stress Rates, Plenum Publ., New York (1973).
11. A. A. Alekseev and B. M. Strunin, "Viscous motion of dislocations in random internal stress fields," in: Dislocation Dynamics [in Russian], Naukova Dumka, Kiev (1975).
12. A. A. Alekseev and B. M. Strunin, "Energy dissipation associated with the motion of a dislocation," Zh. Eksp. Teor. Fiz., 65, No. 6(12) (1973).
13. J. R. Asay and L. M. Barker, "Interferometric measurement of shock-induced internal particle velocity and spatial variations of particle velocity," J. Appl. Phys., 45, No. 8 (1974).
14. A. M. Kosevich, "Dynamic theory of dislocations," Usp. Fiz. Nauk, 84, No. 4 (1964).
15. V. V. Nikolaev, A. N. Orlov, and G. G. Taluts, "Oscillations of a continuum with moving dislocations," Fiz. Met. Metalloved., 23, No. 3 (1967).
16. Yu. I. Meshcheryakov, "Statistical description of the dislocation structure on the basis of the Fokker–Planck equation," ChMMSS, 5, No. 1 (1974).
17. Sh. Kh. Khannanov, "Kinetics of continuously distributed dislocations," Fiz. Met. Metalloved., 46, No. 4 (1978).
18. J. A. Gorman, D. S. Wood, and T. Vreeland, "Mobility dislocations in aluminium," J. Appl. Phys., 40, No. 2 (1969).

ENERGY LOSS BY PLASTIC DEFORMATION IN RADIAL COMPRESSION OF A CYLINDRICAL SHELL

V. G. Belan, S. T. Durmanov,
I. A. Ivanov, V. F. Levashov,
and V. L. Podkovyrov

UDC 538.69

INTRODUCTION

During radial compression of a cylindrical liner at a velocity $\leqslant 10^3$ m/sec, its motion differs from that computed by the equations of ideal fluid hydrodynamics. Agreement can be achieved within the limits of measurement error between experimental data and computation if the energy loss by deformation is taken into account [1]. As in this paper, the behavior of a liner fabricated from a homogeneous and isotropic material is considered in [1]. Its length is assumed constant and so large that edge effects can be neglected, and consideration limited to a ring of unit width. In such a formulation the problem of shell wall deformation is equivalent to their uniaxial compression.

The equation of radial axisymmetric motion of a thin liner subjected to external pressure p(t) has the form [1]

$$\rho h\ddot{R} = N/R - p, \tag{1}$$

where $N = \sigma h$ is the circumferential membrane force, σ is the stress in the liner material, h is the shell wall thickness, $W = (R_0 - R)$ is their displacement, R is the radius of the middle

Moscow. Translated from Zhurnal Prikladnoi Mekhaniki i Tekhnicheskoi Fiziki, No. 2, pp. 109-115, March-April, 1983. Original article submitted January 22, 1981.

 0021-8944/83/2402-0236$07.50

surface, R_0 is its initial value, and ρ is the material density. Several versions of the solution of (1) are examined in [1] for different deformation models taking account of the dependence of the stress σ on the magnitude of the strain $u = W/R_0$. It is shown that by formally varying the parameters in the dependence, agreement between computation and experiment is always achieved successfully. The parameters themselves do not remain constant for the different compression modes, which does not permit computation of liner motion prior to conducting the experiment.

The magnitude of the stress and the work of the strain are found from the energy balance [2]. It was assumed that σ remained constant during compression. However, even in this case it is not clear, first, whether utilization of the found value of the stress for other compression regimes is legitimate, and second, how exactly the computed curve will describe the true shell motion.

The purpose of this paper is to confirm the possibility of computing the liner motion under the effect of a known external pressure pulse for different loading regimes. The growth of stress in the metal is here taken into account in both the elastic deformation stage, and its dependence on the magnitude of the strain and the loading rate in the plastic flow. It is assumed that σ is not explicitly dependent on the strain rate.

Formulation of the Problem

It is known from the theory of strength of solids [3, 4] that a loss of strength sets in with a lag with respect to the time of pressure application for pulsed stresses in metals which even exceed significantly the static yield. This results in the fact that at high loading rates the yield can be increased several times.

The time of the beginning of plastic deformation t_1 and the corresponding value of the dynamic yield σ_1 during shell acceleration by a pulsed pressure of arbitrary shape can be determined from the condition of loss of strength by a solid. Several criteria [3, 5] are proposed that yield similar value of t_1 and σ_1. The assumption of cumulative deformation [3] is used in this paper: the metal goes over into the plastic state at the time t_1 for which

$$\int_0^{t_1} dt/t(\sigma) = 1. \tag{2}$$

Here $t(\sigma)$ is the time of plastic flow development under the effect of an instantaneously applied constant stress σ [3]:

$$t(\sigma) = t(\sigma_0)\exp[-(\sigma - \sigma_0)/m\sigma_0], \tag{3}$$

where $t(\sigma_0)$ is the maximum lag corresponding to $\sigma = \sigma_0$, the static yield point, and m is a constant characterizing the properties of the substance. It is assumed that the temperature of the metal is constant.

This latter condition imposes no constraints on the process being studied. This is related to the fact that, as will be shown later, the yield point is always reached in the initial stage of the motion when shell heating can be neglected.

The membrane force N beyond the yield point is determined by the stress [6]

$$\sigma(u) = \sigma_1[ku/u_1 - k + 1]^{1/k}. \tag{4}$$

Here $u_1 = \sigma_1/E$ is the strain corresponding to the time of reaching the dynamic yield point, k is a constant dependent on the properties of the substance, and E is the Young's modulus of the liner material.

In combination with the equation of motion (1), the relationships (2)-(4) permit, in principle, the execution of a computation of liner motion under the effect of a known pressure pulse. However, the possibility of applying these equations in the case of shell compression is not clear since (2) and (3) were verified experimentally only for characteristic times $t_1 \geqslant 10^{-4}$ sec and for a constant value of σ [3], while the dependence (4) was verified for small strains $u \leqslant 0.05$ [6].

In an investigation of liner motion the external pressure, its growth rate, and the magnitude of the strain are substantially higher. In the case of electromagnetic liner acceleration $p \approx 10^8$ Pa, $t_1 \approx 10^{-5}$ sec, and $u \approx 1$ (compression to total collapse). The purpose of this paper was to show the possibility of applying the relationships mentioned to describe liner motion.

Experimental Study of Liner Motion. The diagram of the experimental apparatus is shown in Fig. 1. A 5-kV condenser battery of 0.013 F was discharged into a single-turn solenoid 1 of width 4 cm. The starting inductance of the loop with the liner 2 was 35 nH. A magnetic field with amplitude to 25 T, measured by the magnetic probe 3, was produced in the gap between the liner and the solenoid. The minimal error in measuring the field with the error for probe calibration taken into account was 5%. A shell of the material AB-0 of 7.5-cm outer diameter and 3.5-cm height was used as liner. The initial liner wall thickness h_0 varied between 2 and 4 mm.

In the experiments to study the initial stage of motion, the small shell strains were measured by using a coaxial capacitor whose plates were the liner itself and a rod 4 separated by insulators 5 (vinyl chloride tubes of 1.5-mm diameter). The capacitor was connected through a separating capacitance to a segment of RK-75-4-11 cable 10 m long with source follower input. Together with the cable, the capacitive sensor was charged from a stabilized supply source and disconnected from it directly before start-up. The voltage on the sensor was checked by a digital voltmeter with no worse than 0.2% accuracy.

Evidently, the constant of the measuring capacitor loop should be much greater than the characteristic time of the process. The source follower had the input resistance 75 MΩ. In this case the accuracy of recording the linear displacement would be no worse than 10% for a 22 T accelerating field amplitude for t = 2 μsec.

The liner radial displacements and the voltage change in the measuring capacitor $\Delta V/V_0$ are related by the dependence

$$\Delta V/V_0 = W/[1 + C_1(1 - W/\zeta_0)/C_0]\zeta_0, \tag{5}$$

where C_1 is the capacitance of the connecting cable, C_0 is the initial capacitance of the measuring condenser, and ζ_0 is the initial magnitude of the gap.

The error in signal magnitude caused by components of the measuring capacitor not being concentric is $\approx 0.5\delta/\zeta_0$ (δ is the magnitude of the eccentricity). The system error did not exceed 5% for a selected 1 mm gap and a measured eccentricity of $\delta \leqslant 0.1$ mm. Results of computing the displacement of a liner with 2 mm wall thickness by means of the oscillograms obtained by using (5) are represented by curve 1 in Fig. 2.

In the experiments to investigate liner motion during large strains, the recording of the inner boundary location was executed by using a SFR operating in the time magnifying mode with a 480,000 frames/sec film speed. The beginning of the process was determined to no worse than 2-μsec accuracy. The amplitudes of the instabilities being developed on the inner surface remained small for accelerating fields greater than 21 T, as compared with the radius up to R_1 = 3 mm (R_1 is the radius of the shell inner boundary). A typical oscillogram of the field in the liner-solenoid gap is shown in Fig. 3 (curve 1). The dependence $R_1(t)$ for this case is here represented by the curve 2 for h_0 = 2.5 mm.

Computation of the Initial Stage of Liner Motion. Comparison with Experiment. Considering initially that (2) and (3) are valid under conditions of experiments with liners, we estimate the possible magnitude of the dynamic yield point. For small radial displacements, (1) is converted to the form [6]

$$d^2u/d\tau^2 = pR_0/(h_0E) - \sigma/E, \tag{6}$$

where $\tau = ct/R_0$, $c^2 = E/\rho$. In the general case the liner motion can be computed only by numerical methods. However, for certain dependences $p(\tau)$ an analytical solution of (6) is successfully obtained.

Let us examine the process of shell compression under the effect of an external pressure $p = p_0\tau/\tau_0$ in the elastic strain domain ($\sigma = Eu$). The solution of (6) for zero initial conditions has the form $u = p_0R_0(\tau - \sin\tau)/(h_0\tau_0E)$. For $\tau^2 \ll 20$ we obtain $u \approx p_0c^2t^3/(6t_0R_0h_0E)$ from this equation. Substituting the value $\sigma = Eu = At^3$ in (3), where $A = p_0c^2/6t_0R_0h_0$, we find its corresponding lag $t(\sigma) = t(\sigma_0)\ \exp\ [(\sigma_0 - At^3)/(m\sigma_0)]$. According to (2) the time of the loss of strength in this case is determined from the condition

$$\int_0^{t_1} y(t)\,dt = \int_0^{t_1} \exp\left[At_1^3/(m\sigma_0)\right] dt = t(\sigma_0)\exp(1/m).$$

The integral of the rapidly growing function y(t) that reaches the highest value (but

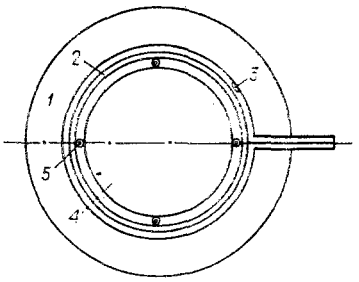

Fig. 1

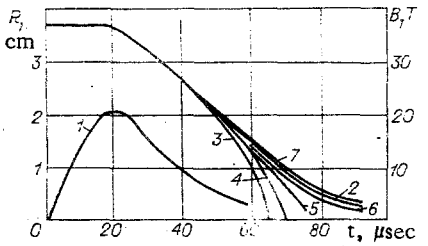

Fig. 2

not the maximum) $y(t_1)$ at one of the ends of the integration range can be estimated by setting it equal to $y^2(t_1)/\dot{y}(t_1)$ [7]. It follows from the solution obtained in this manner for the equation for t_1 that the time to reach the dynamic yield point is determined by the expression

$$t_1 = \left(\frac{m\sigma_0}{A}\right)^{1/3}\left\{\ln\left[3t(\sigma_0)\left(\frac{A}{m\sigma_0}\right)^{1/3}\right] + \frac{1}{m}\right\}^{1/3}. \tag{7}$$

Here

$$\sigma_1 = At_1^3 = m\sigma_0\{\ln\left[3t(\sigma_0)(A/m\sigma_0)^{1/3}\right] + 1/m\}. \tag{8}$$

The velocity at the time t_1 reaches the quantity

$$\dot{u}(t_1) = 3\sigma_1/(Et_1) = 3u_1/t_1. \tag{9}$$

Results of calculating σ_1/σ_0 (curve 1), t_1 (curve 2), and $\dot{u}(t_1)$ (curve 3) by means of (7)-(9) are represented in Fig. 4 for an aluminum liner ($\sigma_0 = 8\cdot10^7$ Pa, m = 0.043, $c = 5\cdot10^3$ m/sec, $t(\sigma_0) = 4\cdot10^8$ sec [3]) with $R_0 = 5$ cm, $h_0 = 2$ mm, and $p_0 = 2.5\cdot10^8$ Pa.

It is seen that an increase in the rate of pressure growth (reduction in t_0) results in a diminution in the time t_1 during which plastic deformation develops. The quantity At_1^3 turned out to be such that the value of σ_1 depends weakly on the loading rate in the range of t_0 variation between 10^{-5} and $2\cdot10^{-4}$ sec that is typical for experiments with liners.

The initial stage of liner motion in the experiments described above was also computed by means of (6), which was solved numerically. The pressure $p(\tau)$ was evaluated from the instantaneous values of the magnetic field in the liner–solenoid gap for each experiment. The insignificant field diffusion in the liner cavity was neglected.

The stress $\sigma_i = Eu_i$ and its corresponding value of t_i from (3) were determined in the first stage of the computations in the elastic strain domain at each step of the integration, and the sum $\sum_{j=1}^{i} \Delta t/t_j(\sigma)$, was evaluated, where $\Delta t = \Delta\tau R_0/c$, $\Delta\tau$ is the constant integration spacing. The computation was halted as soon as the sum mentioned, that corresponds to the integral (2), reached a quantity close to one with a deviation to either side of not more than 10% within the limits of a spacing.

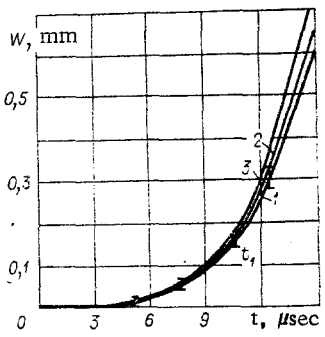

Fig. 3

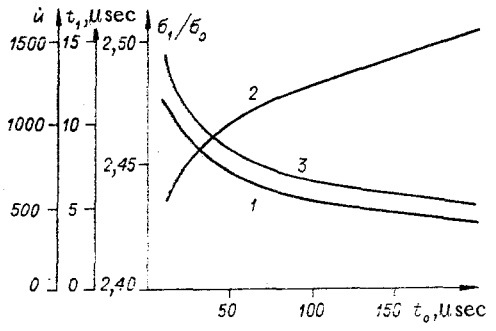

Fig. 4

Starting with the time $\tau_1 = ct_1/R_0$, Eq. (6) was solved for $\sigma(u)$ determined from (4). The values of u_1 and $\dot{u}(t_1)$ from the solution in the elastic strain domain were the initial conditions. The computed dependence of the displacement of the inner boundary of a liner with a 2 mm wall thickness is displayed by the curve 2 in Fig. 2. The point t_1 corresponds to the time the dynamic yield point reaches $\sigma_1 = 2 \cdot 10^8$ Pa. The computed displacements turned out to be higher than the measured values for all values of the above-mentioned range of liner wall thicknesses; however, this difference is not outside the limits of experimental error.

Curve 3 in Fig. 2 corresponds to the results of computations with the Prandtl rheological model [8] in which $\sigma = Eu$ is assumed for $u \leqslant \sigma_0/E$ and $\sigma = \sigma_0 = \text{const}$ for $u > \sigma_0/E$. The difference between this curve and the experimental curve substantially exceeds the measurement error. The data obtained confirm the possibility of applying known methods of computing the behavior of aluminum under conditions typical for electromagnetic acceleration of liners that are characterized by a loading rate to $2 \cdot 10^{13}$ Pa/sec with a front $\sim 10^{-5}$ sec.

Starting from the value of the dynamic yield point found above, the energy loss by strain during compression of an aluminum liner can be computed.

Computation of Liner Motion Under Large Deformation. Comparison with Experiment. The equation of axisymmetric strain of a shell layer has the form [9]

$$\left(\frac{\partial \dot{r}}{\partial t} + \dot{r}\frac{\partial \dot{r}}{\partial r}\right)\rho = -\frac{\partial \sigma_r}{\partial r} + \frac{(\sigma_\theta - \sigma_r)}{r},$$

where σ_r, σ_θ are the radial and tangential stresses. For $\sigma_\theta = \sigma_r$ it describes ideal fluid liner motion. Compression of a cylinder from elastic–plastic material is accompanied by energy accumulation during elastic strain and loss during plastic. In this case the condition $\sigma_\theta - \sigma_r = \sigma > 0$ should evidently be satisfied. We assume the stress σ, which governs the magnitude of the energy expenditure in liner deformation, equals Eu under elastic compression and may be found from the relationship (4) with $u = [R_1(0) - R_1]/R_1(0)$ beyond the yield point ($R_1(0)$ is the initial value of R_1).

Taking account of the incompressibility of the substance (ρ = const and σ is constant over the liner section) in integrating the equation of motion of a thin layer with respect to r between R_1 and R_2, we obtain

$$\ddot{R}_1 = \frac{\sigma}{\rho R_1} - \frac{\dot{R}_1^2}{R_1}\left[1 - \frac{S_0}{(S_0 + R_1^2)\ln\left(1 + S_0/R_1^2\right)}\right] - 2\frac{p_2 - p_1}{\rho R_1 \ln\left(1 + S_0/R_1^2\right)}. \qquad (10)$$

Here p_2 is the pressure on the cylinder outer boundary, p_1 the pressure on the inner boundary, $S_0 = R_2^2(0) - R_1^2(0)$, $R_2(0)$ is the initial value of the outer shell radius R_2. At the time t = 0 we have $R_1(0) = R_0 - h_0/2$ and $\dot{R}_1(0) = 0$. In deriving (10) we assumed σ constant over the liner section at any time. The maximal difference in the magnitude of the stress σ occurs on the shell boundaries during complete collapse. Using (4) it can be shown that for $h_0/R_0 = 0.05$ and $k = 16.5$ [6], at this time $\sigma(R_2)/\sigma(R_1) = [1 - \sqrt{S_0/R_2^2(0)}] = 0.02$. To such accuracy is $\sigma(r) = \text{const}$ taken over the section.

The validity of the assumptions made above can be verified by comparing experimental results with the computation of liner motion by means of (10).

This equation was solved numerically. The time of the passage into the plastic state is found exactly as in computations to determine the dynamical yield point. The computations were executed for different dependences $\sigma(u)$: 1) $\sigma = 0$; 2) $\sigma = Eu$ in the elastic strain

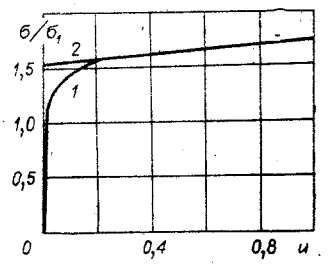

Fig. 5

TABLE 1

R_0/h_0	$\dot{R}(0)\cdot10^{-3}$, m/sec	$Q_0\cdot10^{-5}$, J/m	Computation by equation of motion (10): a, cm	Computation by equation of motion (10): η	Computation by (11), (12): a, cm	Computation by (11), (12): η
20	0,25	0,66	3,4	1,00	3,0	1,00
	0,50	2,65	1,2	1,00	1,0	1,00
	0,75	5,96	0	0,63	0	0,74
	1,00	10,6	0	0,35	0	0,42
	1,25	16,6	0	0,23	0	0,27
	1,50	23,8	0	0,16	0	0,18
40	0,25	0,33	3,6	1,00	3,2	1,00
	0,50	1,32	1,4	1,00	1,1	1,00
	0,75	3,0	0	0,81	0	0,90
	1,00	5,3	0	0,46	0	0,50
	1,25	8,3	0	0,29	0	0,32
	1,50	11,9	0	0,20	0	0,22
60	0,25	0,22	3,65	1,00	3,2	1,00
	0,50	0,88	1,5	1,00	1,2	1,00
	0,75	2,0	0	0,90	0	0,99
	1,00	3,5	0	0,51	0	0,55
	1,25	5,5	0	0,33	0	0,35
	1,50	8,0	0	0,23	0	0,25

domain and $\sigma = \sigma_0[ku/u_1 - k + 1]^{1/k}$ outside the yield point; 3) $\sigma = \sigma_1$; 4) $\sigma = Eu$ for $u \leq \sigma_1/E$ and $\sigma = \sigma_1[ku/u_1 - k + 1]^{1/k}$ for $u > \sigma_1/E$.

The instantaneous value of the pressure $p_2(t)$ was determined, as before, by means of oscillograms of the magnetic field in the liner–solenoid gap for each experiment, and p_1 was taken at zero. Results of calculations for the induction of the accelerating field are represented in Fig. 3 by curves 3-6, respectively. It follows from a comparison of experimental and computational data that the solution of (10) with $\sigma(u)$ determined by condition (4) (curve 6), describes the liner motion most accurately.

Using the relationship (2)-(4), (10) the motion pattern of a shell subjected to external motion can be obtained. It is seen from the behavior of the dependence $\sigma(u)$ constructed according to (4) that the main shell strain occurs (for $u > 0.2$) for σ varying weakly according to a linear law in practice (curve 1 in Fig. 5). The dependence 7 in Fig. 3 corresponds to a computation of inner boundary motion with $\sigma = 1.55\sigma_1(1 + 0.1u)$ (curve 2 in Fig. 5). Comparing the curve 7 with experiment shows that the solution of (10) with the simplified dependence $\sigma(\dot{u})$ describes shell compression satisfactorily.

Taking this into account, an expression can be obtained for estimates of the strain energy loss just as is done in [2]. For a liner whose inner boundary $R_1(0)$ is compressed to R_1, they are per unit length

$$Q = -0.75\pi\sigma_1\{1,1[R_2^2(0)\ln((S_0 + R_1^2)/(R_2^2(0)) - R_1^2(0)\ln R_1^2/R_1^2(0) - (R_1^2(0) - R_1^2)\ln((S_0 + R_1^2)/R_1^2)] + 0.2[R_2(0)\times \times \sqrt{S_0 + R_1^2} - R_1(0)R_1 - (R_1^2(0) - R_1^2)\ln((R_2(0) + \sqrt{S_0 + R_1^2})/(R_1(0) + R_1))]\}. \quad (11)$$

Upon total collapse of the shell ($R_1 \to 0$) with initial energy $Q_0 = \pi\rho S_0\dot{R}_1^2(0)/2$, the relative magnitude of the loss equals ($R_0 \gg h_0$)

$$\eta = Q/Q_0 = 1.7\sigma_1(1 + \ln(R_0/2h_0))/[\rho\dot{R}_1^2(0)]. \quad (12)$$

For a liner moving by inertia ($p_2 = p_1 = 0$) at the initial rate $\dot{R}_1(0)$, η can be determined from the results of computations using (10) by setting $\eta = (Q_0 - Q_1)/Q_0$, where Q_1 is the kinetic energy of the shell at the time under consideration.

Presented in the table are data of computations in the range of the initial velocities $\dot{R}(0) = (0.25\text{-}1.5)\cdot10^{-9}$ m/sec with $R_0/h_0 = 20$, 40, 60 for $R_0 = 5$ cm for $p_2 = p_1 = 0$. If it followed from the computation that the liner should be halted at the finite radius a, then η is taken equal to 1. Given in the same table are estimates of the half radius a and the magnitudes of the energy losses η determined from (11) and (12). The ratio of the energy loss

by strain and the initial kinetic energy of the liner is independent of R_0 but is governed by the ratio R_0/h_0, the value of the initial compression rate $\dot{R}(0)$, and the magnitude of the dynamic yield point. Estimates executed by means of (11) and (12) are in good agreement with the computation results according to the equation of motion.

In conclusion, we note the following.

1. Comparison of the results of calculations with the experiments conducted confirms the feasibility of using relationships (2), (3), and (4) for the determination of the characteristics of motion of a liner and the computation of energy loss by deformation.

2. The magnitude of the dynamic limit point of aluminum, in experiments with liners under conditions typical for electromagnetic acceleration, was a constant and uniform $2 \cdot 10^8$ Pa.

3. The energy loss by deformation, determined according to expression (12), in the interval $R_0/h_0 = 20\text{-}60$ for $R(0) = (0.25\text{-}1.5) \cdot 10^3$ m/sec, coincides well with the estimate from the solution of equation (10).

LITERATURE CITED

1. V. P. Knyazev and G. A. Shneerson, "Investigation of fast broadening of thin-walled metal cylinders in a strong magnetic field," Zh. Tekh. Fiz., 40, No. 2 (1970).
2. F. Herlach and J. E. Kennedy, "The dynamics of imploding liners in magnetic flux compression experiments," Appl. Phys., 6 (1973).
3. V. R. Regel', A. I. Slutsker, and É. E. Tomashevskii, "Kinetic nature of the strength of solids," Usp. Fiz. Nauk, 106, No. 2 (1972).
4. S. N. Zhurkov and É. E. Tomashevskii, "Time dependence of the strength for different loading modes," Certain Problems of the Strength of a Solid [in Russian], Izd. Akad. Nauk SSSR, Moscow (1959).
5. M. S. Kachan and Yu. A. Trishin, "Tensile stresses in a target during the collision of solids," Zh. Prikl. Mekh. Tekh. Fiz., No. 4 (1977).
6. M. J. Forrestal and H. C. Walling, "Axisymmetric plastic response of rings to short-duration pressure pulses," AIAA J., 10, No. 10 (1972).
7. Ya. B. Zel'dovich and A. D. Myshkis, Elements of Applied Mathematics [in Russian], Nauka, Moscow (1967).
8. D. Bland, Theory of Linear Viscoelasticity [Russian translation], Mir, Moscow (1965).
9. W. Prager, Introduction to the Mechanics of Continuous Media [Russian translation], IL, Moscow (1963).

RESIDUAL STRESSES AND VISCOSITY IN THE HIGH-SPEED DEFORMATION OF METALS

N. N. Sergeev-Al'bov

UDC 539.376

By formulating a numerical experiment, the residual stresses occurring in the surface layer of a metal after the passage of a pressure pulse are studied in this paper. Their magnitude as a function of the magnitude and rate of traversal of the acting pressure pulse is studied. The stressed behavior of the metal is described by Maxwell equations of a linear viscoelastic medium [1]. Taking account of plastic phenomena occurs in this model because of the introduction of a nonlinear dependence of the relaxation time on the tangential stress intensity.

To describe metal behavior under high-speed strain, a viscous incompressible fluid model is often used. Within the framework of this model, the viscosity of metals during collisions in the explosive welding mode is investigated in [2]. Here the model equation utilized in [2] and the Maxwell model are compared in an example of numerical results.

Novosibirsk. Translated from Zhurnal Prikladnoi Mekhaniki i Tekhnicheskoi Fiziki, No. 2, pp. 116-121, March-April, 1983. Original article submitted February 9, 1982.

0021-8944/83/2402-0242$07.50